Photonic force spectroscopy on metallic and absorbing nanoparticles

Patrick C. Chaumet
Institut Fresnel (UMR 6133), Université d'Aix-Marseille III, Avenue Escadrille Normandie-Niemen, F-13397 Marseille Cedex 20, France

Adel Rahmani
Laboratoire d'Electronique, Optoélectronique et Microsystèmes, UMR CNRS, 5512 Ecole Centrale de Lyon 36, avenue Guy de Collongue, F-69134 Ecully Cedex, France

Manuel Nieto-Vesperinas
Instituto de Ciencia de Materiales de Madrid, Consejo Superior de Investigaciones Cientificas, Campus de Cantoblanco, Madrid 28049, Spain

(Received 18 March 2004; revised manuscript received 9 July 2004; published 26 January 2005)

We present a detailed study of the optical trapping and manipulation of nanoparticles with complex permittivity using an apertureless near-field probe. We use a three-dimensional, self-consistent description of the electromagnetic scattering processes that accounts for retardation and the intricate many-body interaction between the substrate, the particle, and the probe. We analyze the influence of absorption on the optical force. For metals we describe how the optical force spectrum is influenced by the optical response of the metal, and in particular by plasmon resonances. We find that the optical force spectrum can provide an intrinsic signature of the particle composition which can be used to achieve a material-selective trapping and nanomanipulation.

DOI: 10.1103/PhysRevB.71.045425 PACS number(s): 78.70.−g, 03.50.De, 42.50.Vk

I. INTRODUCTION

Since the pioneering work of Ashkin,[1,2] the use of optical forces has led to the development of optical tweezers techniques which use light to manipulate dielectric particles larger than the wavelength.[3–5] On the other hand, schemes to trap and manipulate nanometric objects in a controlled and selective manner are still scarce. In a previous article,[6] we proposed a scheme to *selectively manipulate* dielectric nanoobjects on a flat dielectric substrate in air or vacuum. This manipulation was achieved using the scattering of evanescent waves at the apex of an apertureless near-field probe. However, that study was restricted to lossless dielectric particles.

The case of metallic particles is more complex due to the imaginary part of the relative permittivity and the existence of plasmon resonances. For large particles (compared to the wavelength of illumination), a two-dimensional optical trap can be created under special conditions, i.e., using TEM_{00} and TEM_{01}^{*} laser modes.[7,8] But it is only very recently that large metallic particle have been trapped in three dimension.[9,10] In the case of small particles, i.e., particles smaller than the wavelength (Rayleigh particles), the optical trapping can be achieved in three dimensions.[11–13] The large interest of small metallic particles is their plasmon resonance which produces an enhancement of the optical force experienced by the particle. This can be used in photonic force microscopy[14] or to trap single molecules to study surface-enhanced Raman scattering.[15]

In this article, using the selective trapping scheme proposed in Refs. 6 and 16, we extend the analysis of our optical trap to the selective manipulation of absorbing and metallic particles. The optical trapping of dielectric particles is the result of the gradient force only, as the scattering force is negligible, compared to this gradient force, for small particles. However, absorbing and metallic particles, due to the nonzero imaginary part of their relative permittivity, experience an absorbing force of the same order of magnitude as the gradient force. We shall investigate the consequences of this force on the stability of the optical trap. Moreover, we shall address the effect of the plasmon resonance of small particles on the optical forces.

Since the details of the computation of optical forces have been described previously,[17–19] only a brief account of the theory is given in Sec. II. Section III A presents the results for absorbing dielectric particles (e.g., quantum dots). Section III B addresses the case of metallic particles. The influence of plasmon resonances on the optical trapping is discussed, with a particular emphasis on the case of silver particles which exhibit an intricate behavior. In Sec. III C we study the possibility of scanning the surface in tapping mode with a metallic particle trapped at the tip apex. Finally, we present our conclusions in Sec. IV.

II. CALCULATION OF THE OPTICAL FORCES

We use the coupled dipole method (CDM) to compute the optical forces. The method consists in discretizing the object under study as a set of polarizable subunits arranged on a cubic lattice. As the incident field ($\mathbf{E}_0$) is time-harmonic-dependent, we shall omit the frequency dependence. The field at each subunit is obtained by the following self-consistent relation:

$$\mathbf{E}(\mathbf{r}_i) = \mathbf{E}_0(\mathbf{r}_i) + \sum_{j=1}^{N} [\mathbf{T}(\mathbf{r}_i,\mathbf{r}_j) + \mathbf{S}(\mathbf{r}_i,\mathbf{r}_j)]\alpha(\mathbf{r}_j)\mathbf{E}(\mathbf{r}_j), \quad (1)$$

where $\alpha(\mathbf{r}_j)$ is the polarizability of subunit j, $\mathbf{T}$ is the electric field linear susceptibility in free space,[20] and $\mathbf{S}$ denotes the

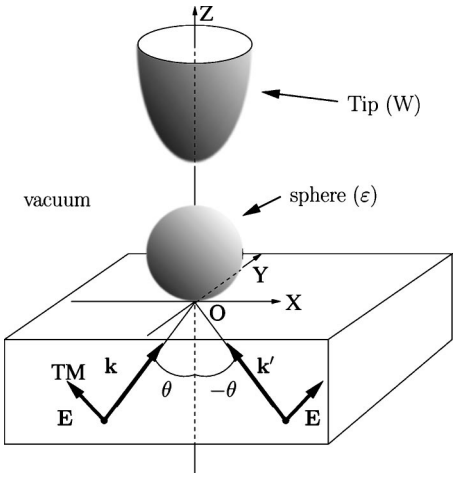

FIG. 1. Schematic of the configuration. A sphere on a flat dielectric surface is illuminated under total internal reflection, i.e., $\theta > \theta_c$ with $\sqrt{\epsilon}\sin(\theta_c)=1$. A tungsten probe is used to create an optical trap. The illumination can be done either in TM polarization (as drawn in the figure) or in TE polarization.

field linear susceptibility in the presence of a substrate.[21] The polarizability contains the radiative reaction term which ensures that the optical theorem is satisfied.[22,23] Since we are dealing with optical frequencies, we need to compute the time-averaged force. This net force on one subunit is[23]

$$F_u(\mathbf{r}_i) = (1/2)\mathrm{Re}\left(\sum_v p_v(\mathbf{r}_i)\frac{\partial[E^v(\mathbf{r}_i)]^*}{\partial u}\right), \tag{2}$$

where u or v stands for either x, y, or z, $\mathbf{p}(\mathbf{r}_i)$ is the electric dipole moment of the ith subunit, and $*$ denotes the complex conjugate. Notice that the derivative of the electromagnetic field is obtained by differentiation of Eq. (1) with respect to the vector $\mathbf{r}_i$. Hence, the net optical force on the object is obtained as

$$\mathbf{F} = \sum_{i=1}^{N} \mathbf{F}(\mathbf{r}_i). \tag{3}$$

III. RESULTS

Consider a particle with complex relative permittivity $\varepsilon = \varepsilon_r + i\varepsilon_i$ placed in air above a flat dielectric substrate (relative permittivity $\epsilon = 2.25$). The particle is illuminated by two evanescent waves created by the total internal reflection of plane waves at the substrate/air interface ($\theta > \theta_c = 41.8°$ with $\sqrt{\epsilon}\sin\theta_c = 1$). These two waves are counterpropagating evanescent waves, i.e., $\mathbf{k}_\parallel = -\mathbf{k}'_\parallel$, with the same polarization and a random-phase relation (Fig. 1, see Ref. 16 for the more details). The irradiance due to the laser illuminating the surface is taken to be 0.05 $\mathrm{W}/\mu\mathrm{m}^2$.[16]

A. Absorbing particles

In this section we consider an absorbing particle with radius $a = 10$ nm and $\mathrm{Re}(\varepsilon) = 2.25$. We shall study the influence of the complex relative permittivity on the trapping and nanomanipulation process. The trapping is performed with a tungsten tip of radius at the apex $r = 10$ nm. The wavelength is $\lambda = 514$ nm. The angle of incidence for the illumination is chosen to be $\theta = 43°$; this is the angle at which the optical potential is deepest.[16] We recall briefly here the procedure used to manipulate a particle; the procedure has been described in detail for dielectric particles in Refs. 6 and 16 and it remains the same in the case of absorbing or metallic particles. In TE polarization, the probe scans the surface to localize the particles. In that case the optical force is always negative. Then the polarization is switched to TM and the optical force becomes positive when the tip is close (a few nanometers) to the particle. Once the particle is trapped at the apex of the tip, it can be manipulated and subsequently released by switching back to TE polarization.

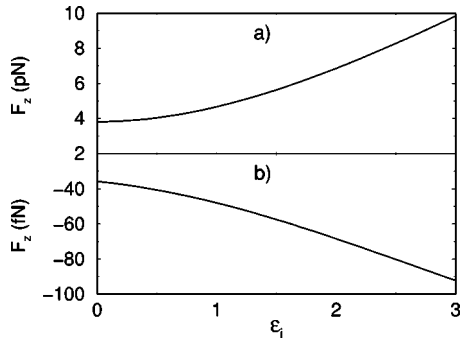

FIG. 2. z component of the force experienced by an absorbing sphere [$\mathrm{Re}(\varepsilon) = 2.25$] vs the imaginary part of the relative permittivity. The tungsten tip is in contact with the sphere and the angle of incidence is $\theta = 43°$. (a) TM polarization. (b) TE polarization.

Figure 2 shows the z component of the force experienced by the sphere, for the two polarizations, when the imaginary part of the relative permittivity increases [Fig. 2(a), transverse magnetic (TM) polarization, and Fig. 2(b), transverse electric (TE) polarization] and the tip is in contact with the sphere. For both polarizations, the magnitude of the force is enhanced when the imaginary part of the relative permittivity increases. For a better understanding of this effect, let us decompose the polarizability α of a small sphere (compared to the wavelength of illumination) into its real and imaginary parts,[24]

$$\mathrm{Re}(\alpha) = a^3\frac{(\varepsilon_r - 1)(\varepsilon_r + 2) + \varepsilon_i^2}{(\varepsilon_r + 2)^2 + \varepsilon_i^2}, \tag{4}$$

$$\mathrm{Im}(\alpha) = a^3\frac{3\varepsilon_i}{(\varepsilon_r + 2)^2 + \varepsilon_i^2}, \tag{5}$$

where a is the radius of the sphere. For our geometry the z component of the optical force on the small sphere is mainly due to the gradient force[25] which is proportional to the real part of the polarizability of the sphere. From Eq. (4) it is obvious that when ε_i increases, the real part of the polarizability increases and so does the gradient force, hence the force becomes more positive for TM polarization, and more negative for TE polarization. Note that as ε_i becomes very large, $\mathrm{Re}(\alpha)$ tends toward a finite limit.

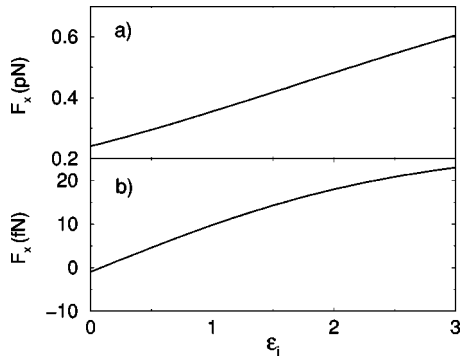

FIG. 3. Lateral (x) component of the force experienced by an absorbing sphere [$\mathrm{Re}(\varepsilon)=2.25$] vs the imaginary part of the relative permittivity if the symmetric illumination is not used. The tungsten tip is in contact with the sphere, $\theta=43°$. (a) TM polarization. (b) TE polarization.

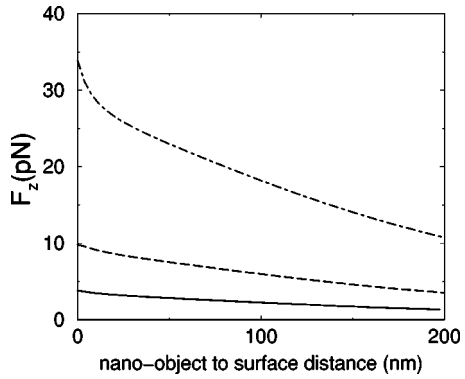

FIG. 4. z component of the force experienced by the sphere as a function of the distance between the sphere and the substrate for TM polarization. The sphere is placed at the apex of the probe. $\theta=43°$. Solid line $\varepsilon=2.25$, dashed line $\varepsilon=2.25+3i$, dot-dashed line $\varepsilon=12.5+i$.

Figure 3 shows the lateral force experienced by the sphere for both polarizations if only one laser beam is used for the illumination. The force is plotted for the case $\mathbf{k}_{\parallel}>\mathbf{0}$ (illumination from the left side of Fig. 1). We note that for both polarizations, the lateral optical force is never zero and therefore it should be difficult to trap a particle with a single beam illumination. The symmetric illumination prevents the sphere from escaping from the optical trap.[19] For TM polarization, the increase of the absorption only gives an enhancement of the lateral force as the two forces—the gradient force and the absorbing force—are both positive (the gradient force is positive because the maximum of the intensity of the electromagnetic field is obtained slightly to the right of the tip apex due to the nonsymmetric illumination). But for TE polarization the behavior is different because the sign of the lateral force changes. When the absorbing part of the relative permittivity vanishes, only the (negative) gradient force remain (the scattering force is negligible due to the small size of the particle compared to the wavelength of illumination). Conversely to the TM polarization, for TE polarization the minimum of the intensity of the electromagnetic field is obtained slightly to the left of the tip apex which produces a negative gradient force. But when the imaginary part of the polarizability increases, there appears an absorbing force. This absorbing force comes from the incident evanescent wave which propagates parallel to the substrate. Due to the choice of illumination, this force is positive. Because the lateral gradient force is weak, it is easily outweighed by the absorbing force which yields the main contribution. This is why a large, positive lateral force exists in this case.

Since we have shown (Fig. 3) the importance of using a symmetric illumination, all the following computations will be done in that case. Figure 4 shows the z component of the force when the sphere is lifted by the probe (the sphere is placed at the tip apex). We have plotted the results for three values of the relative permittivity: a lossless dielectric sphere with $\varepsilon=2.25$ (which is our reference), and two absorbing spheres with $\varepsilon=2.25+3i$ and $\varepsilon=12.5+i$, respectively. A comparison of the lossless sphere case (solid line) and the absorbing case (dashed line) shows that a nonzero imaginary part of the relative permittivity increases the force experienced by the sphere, and hence it helps trap and manipulate the particle. In the case of $\varepsilon=12.5+i$, due to the large real part of the polarizability, the z component of the force is clearly stronger than in the two previous cases. But a closer look at the curves shows that the z component of the force is not directly proportional to $\mathrm{Re}(\alpha)$. We have for $\varepsilon=2.25$, $\mathrm{Re}(\alpha)=0.3a^3$; for $\varepsilon=2.25+3i$, $\mathrm{Re}(\alpha)=0.5a^3$; and for $\varepsilon=12.5+i$, $\mathrm{Re}(\alpha)=0.8a^3$. Between the lossless dielectric sphere and the sphere with $\varepsilon=12.5+i$, the real part of the polarizability is multiplied by 2.6 and the force by a factor 8. The proportionality relation only applies for a sphere in free space. However, due to the strong interaction between the sphere and the tungsten tip, there is a strong enhancement of the field around the tip apex when the relative permittivity of the particle increases. This effect improves the efficiency of the trapping and, therefore, the larger the real part of the polarizability, the easier the manipulation. Notice that although the radius of the trapped sphere is about 10 nm, we have checked that the trapping is achieved up to a radius of 85 nm for the absorbing sphere ($\varepsilon=3+i$). Hence the approach presented here could, for instance, allow one to manipulate quantum-dot nanocrystals and place them into a specific configuration to study dot-dot interactions, or one nanocrystal could be isolated to study single-dot properties.[26]

We have not plotted the force experienced by the sphere versus the distance between the sphere and the tip, nor did we plot the evolution of the optical force as the tip scans the surface above the substrate, because these results are similar to those obtained for dielectric particles.[16] However, we emphasize that it is particularly important to use a symmetric illumination with absorbing particles to avoid the disruptive effect of the lateral force.

B. Metallic particles

In this section, we consider metallic particles which exhibit plasmon resonances, i.e., gold, silver, and copper particles. We shall start by illustrating the convergence of the CDM calculation for a sphere in free space. This problem can be solved exactly in the form of a Mie series which we

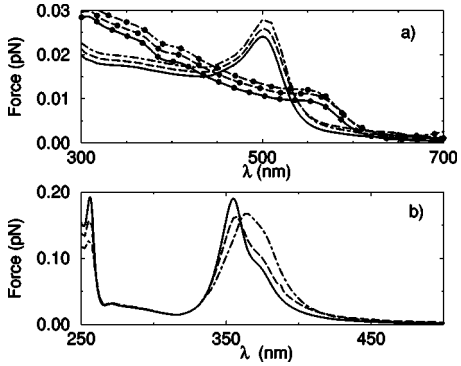

FIG. 5. Force experienced by a sphere with radius $a=10$ nm in free space vs the wavelength of illumination. Solid line: Mie calculation. Dotted line: CDM with $d=4$ nm. Dashed line: CDM with $d=0.95$ nm. (a) Without symbol: gold sphere; circles: copper sphere. (b) Silver sphere.

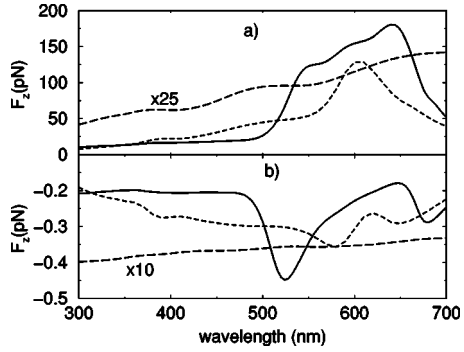

FIG. 6. z component of the force experienced by a sphere of radius $a=10$ nm vs the wavelength of illumination. The tungsten tip is in contact with the sphere. The solid line pertains to a gold sphere, the dotted line a copper sphere, and the dashed line a dielectric sphere. (a) TM polarization. (b) TE polarization.

shall use as a reference. The comparison to the Mie result is done for the three metals studied in this work; the sphere has a radius $a=10$ nm. We plot in Fig. 5(a) the optical force for the gold and copper spheres. The Mie results are plotted with a solid line. The other curves pertain to the CDM. With a dotted line we plot the result computed with $d=4$ nm, and with a dashed line the force computed with $d=0.95$ nm. It is obvious that when d decreases, the force computed with the CDM converges toward the Mie result. With $d=4$ nm, the error in the magnitude of the force is small (we slightly overestimate the optical force), hence a lattice spacing of $d=4$ nm is sufficient for our purpose of studying the general physical process of optical trapping and manipulation of metallic particles. For a silver sphere, as shown in Fig. 5(b), again the CDM converge towards the Mie result when d decreases. However, the convergence is slower than for gold or copper. To get a quantitatively accurate representation of the resonance, one should take the smaller discretization, but for the sake of computation time and memory, we shall take $d=4$ nm for the silver as well. Notice that the comparison with Mie is for a sphere in free space. In a more complex geometry, such as ours, the variation of the field is most likely stronger. However, because the sphere is very small and it is discretized, we are taking into account the variation of the field inside the sphere, and we can assume that the degree of convergence of the CDM remains the same in our complex configuration.

Notice that beside the dipole mode, a metallic sphere can support quadrupole or higher electromagnetic modes. Because the sphere is discretized in small subunits, we actually take into account all the multipolar modes of the sphere as described in Ref. 27, hence our force calculation takes into account the multipolar response of the sphere. However, for a small metallic sphere, as in our case, the effect of modes higher than the dipole mode is negligible. One can see in Ref. 28 that for a small metallic sphere (in an evanescent incident field), the plasmon resonance computed with the dipole approximation or with the CDM gives an accurate result. The multipole expansion only changes the magnitude of the scattered field, and therefore no important physics is overlooked by treating the sphere as a dipole.

Figure 6 shows the z component of the force experienced by a sphere versus the wavelength of illumination for both polarizations when the tip is in contact with the sphere and the sphere is lying on the glass substrate (see Fig. 1). The solid line pertains to a gold sphere, while the dotted line is related to a copper sphere. In both cases the sphere has a radius $a=10$ nm. Since the relative permittivity of the tungsten tip depends on the wavelength, the dashed line corresponds to the case of a dielectric sphere with constant permittivity, and shows the influence of the tungsten tip only. We see that in TM polarization, the z component of the force experienced by the dielectric sphere increases with the wavelength λ. This is due to the fact that the imaginary part of the relative permittivity of tungsten increases slowly with λ. For TE polarization, as we have no enhancement of the field at the tip apex, the force is less sensitive to the slow variation of the relative permittivity of tungsten. For the gold sphere, and for TM polarization, we find a very strong enhancement of the z component of the force for $\lambda=643$ nm ($F_z=180$ pN). Notice that the plasmon resonance for a small gold sphere is about $\lambda=520$ nm. This difference is due to the strong coupling between the tungsten tip and the sphere. In fact, we do not have the plasmon resonance of one sphere but a plasmon mode of the cavity formed by the sphere and the apex of the tip, which redshifts the resonance of the sphere.[29] Outside the resonance of the plasmon mode, the force is 20 times weaker, but stays stronger than in the case of a dielectric sphere. For TE polarization, the z component of the force is always negative. We can point out that the force varies little with the wavelength of illumination. Only around $\lambda=520$ nm do we observe a decrease of the force by a factor of 2. This minimum corresponds to the plasmon resonance of the sphere alone. This is due to the lack of field enhancement at the tip apex for TE polarization, which produces a weak coupling between the tip and the sphere. For the copper sphere we have the same behavior; for TM polarization the maximum is at $\lambda=605$ nm, hence the plasmon resonance of the copper sphere is redshifted by the presence of the tip. As for TE polarization, the minimum of the force is found again at the plasmon resonance of a single sphere, i.e., $\lambda=585$ nm.

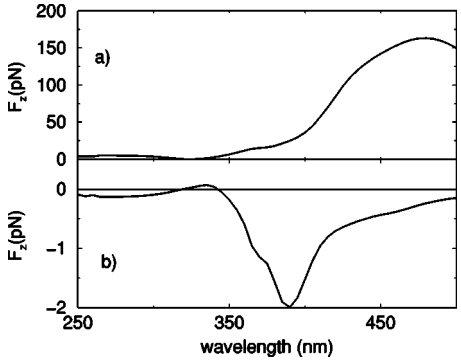

FIG. 7. Same as Fig. 6 but for a silver sphere. (a) TM polarization. (b) TE polarization.

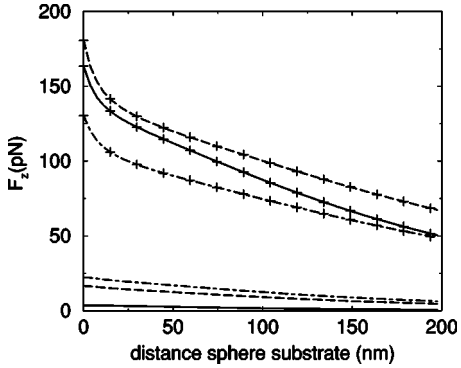

FIG. 8. z component of the force when the sphere is manipulated with the tip. The particle is made of silver (solid line), gold (dashed line), and copper (dot-dashed line). Curves with the "+" marker pertain to forces computed at the plasmon resonance wavelength ($\lambda_{Au}=640$ nm, $\lambda_{Cu}=605$ nm, $\lambda_{Ag}=480$ nm). Curves without a marker are computed away from the plasmon resonance ($\lambda_{Au}=400$ nm, $\lambda_{Cu}=400$ nm, $\lambda_{Ag}=300$ nm).

Figure 7 pertains to a silver sphere ($a=10$ nm). At first the results for the force spectrum are intriguing. For TM polarization, a maximum of the z component of the force is found at $\lambda=480$ nm (the plasmon resonance of a silver sphere is around $\lambda=360$ nm) while the force is close to zero at $\lambda=324$ nm. For TE polarization, we get a range of wavelengths over which a weak positive force along z is obtained, unlike anything we found for gold, copper, or absorbing dielectric particles. To explain the behavior of the silver sphere, let us recall that the gradient force experienced by a small particle in the z direction can be written as

$$F_z = \mathrm{Re}(\alpha)\partial_z|\mathbf{E}|^2/2. \tag{6}$$

Therefore, the sign of F_z depends on the sign of $\mathrm{Re}(\alpha)$. In the case of a dielectric, gold, or copper particle, we have $\mathrm{Re}(\alpha)>0$, which produces, for an incident field evanescent along the z direction, a negative gradient force. For the silver sphere, we have $\mathrm{Re}(\alpha)<0$ in the 316–351 nm spectral range. Therefore, within that range, the sphere experiences from the incident evanescent field a force directed toward regions of lower intensity of the field, that is, away from the substrate (note that at $\lambda=316$ and $\lambda=351$ nm the gradient force on the sphere vanishes as the dipole associated to the sphere is in quadrature with the phase of the incident field). Hence, for silver, the incident evanescent field produces a positive optical force. On the other hand, the interaction between the sphere and the substrate always leads to a negative optical force, irrespective of the dielectric constant of the sphere.[17,18] This force can be understood as the interaction between the dipole associated to the sphere and the reflected field at the dipole location. For a dipole close to a lossless dielectric substrate, the reflected field at the location of the dipole is always in phase with the dipole. This is why the force due to the reflected field is always negative. This is easy to understand as the scattered field at the location of the dipole can be written as

$$\mathbf{E}(\mathbf{r}_i) = \mathbf{S}(\mathbf{r}_i,\mathbf{r}_i)\mathbf{p}(\mathbf{r}_i), \tag{7}$$

where $\mathbf{p}(\mathbf{r}_i)$ is the dipole moment associated with the sphere. Since the dipole is close to the substrate, we can use the static approximation wherein $\mathbf{S}\propto b/z^3$ with z the distance from the dipole to the substrate and b a real positive constant.[17–19] Hence $\mathbf{E}(\mathbf{r}_i)$ is in phase with $\mathbf{p}(\mathbf{r}_i)$ and therefore the gradient force is always negative irrespective of the dipole moment (i.e., the nature of the sphere). Notice that this force is strongest when the dipole moment associated to the sphere is largest, as is the case near the plasmon resonance. As a result, for the silver sphere with a TE polarized incident field, the interaction between the tip and the sphere is weak and the only significant contribution to the optical force experienced by the sphere comes from the interaction with the substrate. Accordingly, a strong negative force is found at $\lambda=385$ nm, which is close to the plasmon resonance of the sphere alone. On the other hand, around $\lambda=320$ nm we have $\mathrm{Re}(\alpha)>0$ and the sphere is attracted toward low-intensity regions, yielding a positive gradient force. However, the modulus of the polarizability is small, which entails a small negative force due to the interaction of the sphere with itself via the substrate. The net force in that case is close to zero. For TM polarization, the explanation is more complex. Due to the field enhancement at the apex of the tip there is a positive contribution to the optical force, but the force remains weak at $\lambda=320$ nm as $\mathrm{Re}(\alpha)\approx 0$ at this wavelength, hence the sum of all the contributions to the gradient force vanishes. We observe a redshift of the maximum of the curve which is now at $\lambda=480$ nm as the plasmon resonance is now a plasmon mode of the cavity shaped by the tip and the sphere. We mentioned previously that when $\mathrm{Re}(\alpha)<0$ (for example, at $\lambda=340$ nm), the sphere is pushed toward low-intensity regions. Therefore, the enhancement of the field at the tip apex in TM polarization should create, in that case, a negative optical force on the sphere, however this is not the case. This is due to the fact that strong evanescent components of the field exist near the tip. As shown in Ref. 18 [see, for instance, Eq. (13)], in the presence of an evanescent field, a sphere close to a dielectric surface (tungsten at the wavelengths we consider in this paper behaves as an absorbing dielectric) will experience a gradient force that will pull it towards the surface irrespective of the nature of the sphere.

In Fig. 8, we present the z component of the force experienced by a gold, silver, or copper sphere at different wave-

lengths (in and out of plasmon resonance) as the sphere is trapped and manipulated by the tip. The behaviors of the three spheres are similar and show that it is easier to manipulate the particle at the plasmon resonance. Notice that the resonance for the three metallic spheres occurs at different wavelengths, and more generally, the behavior of the force versus the wavelength is different. By using the dependence of the force on the spectral response of the sphere, it would be possible to perform a material-selective trapping. For example, at $\lambda = 325$ nm the z component of the force on a silver sphere is close to zero and for this same wavelength the force on the gold sphere is around 12 pN. Hence only the gold sphere would be trapped and manipulated at this wavelength. Finally, we can mention that the decay of the z component of the force with the sphere-substrate distance is different for each curve. This is due to the use of a different wavelength in each case, thus the decay of the evanescent field is different.

When we have many spheres clustered together, for example three identical spheres in contact and aligned following the x axis, we have shown in a previous article that, in the case of dielectric spheres, it is possible to adapt the angle of incidence so as to capture, say, the middle sphere.[16] In the case of metallic spheres it is more complex, as the behavior depends on the wavelength. For three gold spheres, our calculations show that depending on the wavelength, it may or may not be possible only to capture the middle sphere.

C. Apertureless probe with a metallic sphere at the tip apex

We have seen in the previous section that a metallic sphere can be trapped and manipulated at the apex of a tungsten tip. By keeping the same polarization (TM), it should be possible to scan the surface in taping mode, i.e., the tip vibrating perpendicularly to the substrate, in the so-called apertureless scanning near-field optical microscopy mode.[30] Typically, the frequency used in this mode is $f = 4$ kHz with a magnitude for the oscillations $h = 10 - 200$ nm.[30] We take $h = 100$ nm. Assuming a sinusoidal oscillation, $z(t) = h \sin(\omega t)/2$ with $\omega = 2\pi f$, we can compute the z component of the inertial force experienced by the sphere during this oscillation: $F(t) = md^2z(t)/dt^2 = -mh\omega^2 \sin(\omega t)/2$. Hence the maximum force experienced by the sphere is $mh\omega^2/2 = 25$ aN for a gold sphere and 14 aN for a silver sphere. This maximum is always smaller than the optical forces over the distance h (see Fig. 8), even when the particle is manipulated with a wavelength of illumination out of the plasmon resonance, hence it would be possible to scan the surface while keeping the sphere at the tip apex, in spite of the oscillations of the tip. The advantage of scanning the surface with a small metallic sphere as a nanoprobe is to improve the quality of the imaging owing to the increase of the scattered field, as shown in Refs. 31 and 32. Accordingly, at a given operating wavelength, one can choose the nature of the particle trapped at the tip apex such that it yields the largest enhancement of the scattered field. This enhancement yields a better resolution of the near-field microscope. Also, following the resolution wanted one can change also the size of the particle trapped, as the smaller the probe is, the better would be the resolution.

IV. CONCLUSION

In conclusion, we have presented a detailed study of the nanomanipulation of particles with a complex relative permittivity, using an apertureless near-field probe. We considered both absorbing dielectric and metallic particles. In the case of absorbing dielectric particles, such as quantum dots, the presence of an imaginary part in the relative permittivity increases the efficiency (depth) of the optical trap and helps manipulate the particle. In the case of metallic particles, the manipulation is improved if the wavelength of illumination corresponds to the plasmon resonance of the cavity formed by the tip and the particle. We showed that depending on the nature of the metallic sphere, the characteristics of the optical force spectrum are very different. This suggests the possibility of achieving a material selective manipulation. Similarly, the present approach can be applied to the optical manipulation of semiconductor nanoparticles (radius smaller than 100 nm), under an excitonic resonance condition which can increase the optical force as much as four orders of magnitude more than in the absence of excitation.[33]

ACKNOWLEDGMENTS

P.C.C. thanks Kamal Belkebir for many fruitful discussions. A.R. thanks the Ecole Centrale de Lyon BQR program for funding. M.N-V acknowledges grants from the Spanish MCYT and from the EU.

[1] A. Ashkin, Phys. Rev. Lett. **24**, 156 (1970).
[2] A. Ashkin, Phys. Rev. Lett. **25**, 1321 (1970).
[3] R. Holmlin, M. Schiavoni, C. Chen, S. Smith, M. Prentiss, and G. Whitesides, Angew. Chem., Int. Ed. **39**, 3503 (2000); E. R. Dufresne, G. C. Spalding, M. T. Dearing, S. A. Sheets, and D. G. Grier, Rev. Sci. Instrum. **72**, 1810 (2001); E. R. Dufresne and David G. Grier, *ibid.* **69**, 1974 (1998); R. L. Eriksen, V. R. Darias, and J. Glückstad, Opt. Express **10**, 597 (2002); J. Leach, G. Sinclair, P. Jordan, J. Courtal, M. J. Padgett, J. Cooper, and Z. J. Laczik, *ibid.* **12**, 220 (2004).
[4] M. P. Macdonald, L. Paterson, K. Volke-Sepulveda, J. Arlt, W. Sibbet, and K. Dholakia, Science **296**, 1101 (2002).
[5] M. J. Lang and S. M. Block, Am. J. Phys. **71**, 201 (2003).
[6] P. C. Chaumet, A. Rahmani, and M. Nieto-Vesperinas, Phys. Rev. Lett. **88**, 123601 (2002).
[7] S. Sato, Y. Harada, and Y. Waseda, Opt. Lett. **19**, 1807 (1994).
[8] H. Furukawa and I. Yamaguchi, Opt. Lett. **23**, 216 (1998).
[9] M. Gu and D. Morrisk, J. Appl. Phys. **91**, 1606 (2002).
[10] S. A. Tatarkova, A. E. Carruthers, and K. Dholakia, Phys. Rev. Lett. **89**, 283901 (2002).
[11] K. Svoboda and S. M. Block, Opt. Lett. **19**, 930 (1994).
[12] L. Novotny, R. X. Bian, and X. Sunney Xie, Phys. Rev. Lett. **79**,

645 (1997).
[13] A. Rohrbach, H. Kress, and E. H. K. Stelzer, Opt. Lett. **28**, 411 (2003).
[14] J. R. Arias-Gonzàlez, M. Nieto-Vesperinas, and M. Lester, Phys. Rev. B **65**, 115402 (2002).
[15] H. Xu and M. Käll, Phys. Rev. Lett. **89**, 246802 (2002).
[16] P. C. Chaumet, A. Rahmani, and M. Nieto-Vesperinas, Phys. Rev. B **66**, 195405 (2002).
[17] P. C. Chaumet and M. Nieto-Vesperinas, Phys. Rev. B **61**, 14119 (2000).
[18] P. C. Chaumet and M. Nieto-Vesperinas, Phys. Rev. B **62**, 11185 (2000).
[19] P. C. Chaumet and M. Nieto-Vesperinas, Phys. Rev. B **64**, 035422 (2001).
[20] J. D. Jackson, *Classical Electrodynamics*, 2nd ed. (John Wiley, New York, 1975), p. 395.
[21] A. Rahmani, P. C. Chaumet, and F. de Fornel, Phys. Rev. A **63**, 023819 (2001).
[22] P. C. Chaumet, Appl. Opt. **43**, 1825 (2004).
[23] P. C. Chaumet and M. Nieto-Vesperinas, Opt. Lett. **25**, 1065 (2000).
[24] For the sake of simplicity, the radiation-reaction term is omitted.
[25] For a sphere above a surface in an evanescent field, the *z* component of the force is the result of the gradient force only; see Refs. 17 and 18.
[26] P. Michler, A. Imamoğlu, M. D. Mason, P. J. Carson, G. F. Strouse, and S. K. Buratto, Nature (London) **406**, 968 (2000).
[27] C. Bourrely, P. Chiappetta, T. Lemaire, and B. Torresani, J. Opt. Soc. Am. A **9**, 1336 (1992).
[28] P. C. Chaumet, A. Rahmani, F. de Fornel, and J.-P Dufour, Phys. Rev. B **58**, 2310 (1998).
[29] P. C. Chaumet, Ph.D. thesis, Université de Bourgogne, France (1998).
[30] G. Wurtz, R. Bachelot, and P. Royer, Eur. Phys. J.: Appl. Phys. **5**, 269 (1999).
[31] M. Gu and P. C. Ke, Opt. Lett. **24**, 74 (1999).
[32] T. Kalkbrenner, M. Ramstein, J. Mlynek, and V. Sandoghdar, J. Microsc. **202**, 72 (2001).
[33] T. Iida and H. Ishihara, Phys. Rev. Lett. **90**, 057403 (2003).